

# FSO Detection Using Differential Signaling in Outdoor Correlated-Channels Condition

Mojtaba Mansour Abadi, Zabih Ghassemlooy, Mohammad-Ali Khalighi, Stanislav Zvanovec, and Manav R. Bhatnagar

**Abstract**—In this paper, we introduce a detection technique based on differential signaling scheme for outdoor free space optical communications. This method requires no channel state information (CSI) and does not suffer from the computational load compared to conventional receivers, where adjusting dynamically the detection threshold level (either based on CSI knowledge, or by using pilots) leads to increased computational time and reduced link throughput. This paper shows that the performance of the proposed technique only depends on the correlation of propagating optical beams. Especially under highly correlated-channels condition the fluctuation of the detection threshold level in the receiver is significantly small. We also show experimentally that under weak turbulence regime the variance of detection threshold level reduces for the correlated channel.

**Index Terms**—Optical communication; free space optics (FSO); adaptive threshold detection; channel estimation; atmospheric turbulence.

## I. INTRODUCTION

THE received signal in free space optical (FSO) communication systems is highly sensitive to the atmospheric effects such as fog, smoke, low clouds, snow, rain and the atmospheric turbulence (AT) [1-4] that may result in severe power loss and channel fading. In non-return-to-zero on-and-off keying (NRZ-OOK) intensity-modulation/direct-detection (IM/DD) systems, an optimal detection threshold level (DTL) at the receiver can be used to distinguish the received '0' and '1' bits. However, under AT, the FSO link experiences fading, which can cause the received signal power to drop below the receiver's threshold for milliseconds at a time, thus leading to the random fluctuation of the optimal

DTL. Since these optical power fades are often very deep, simply increasing the transmit power  $P_t$  and using a fixed optimal DTL in this case would not be effective [2].

Most already-proposed detection methods rely on the knowledge of instantaneous or statistical CSI. For instance, to resolve the fluctuation of DTL, in [5] the maximum-likelihood sequence detection (MLSD) scheme was adopted, and it was shown that provided the temporal correlation of AT  $\tau_0$  is known MLSD outperforms the maximum-likelihood (ML) symbol-by-symbol detection technique. In practical applications  $\tau_0 \cong 1 - 10$  ms; then, to maximize the link performance,  $\tau_0$  needs to be adjusted dynamically. In addition, MLSD suffers from high computational complexity. In [6] two sub-optimal MLSD schemes, based on the single-step Markov chain model, were proposed to reduce the receiver computational complexity; however they still require CSI knowledge. By pilot symbol (PS) assisted modulation (PSAM), assuming that  $\tau_0$  is known, CSI is acquired by inserting some PS to the data [7]. However, obtaining an accurate-enough instantaneous CSI necessitates a non-negligible pilot overhead. Recently an ML based sequence receiver, requiring no prior knowledge of CSI or channel model was proposed in [1] with the capability of dealing with various fading conditions. However, the system suffers from high implementation complexity. In order to use in commercial FSO products, it is desirable to employ low complexity signal detection with simple data framing and packetization to ensure infrastructure transparency [8].

In outdoor FSO links, differential signaling (DS) was used in [9] to remove the effect of background noise. Also the same idea was adopted in [2] that used a pre-fixed optimal DTL for various atmospheric channel conditions (rain, AT, etc.). The detection technique did not relied on CSI (with increased computational load at the receiver) and PS or a training sequence [2]. However, their simulation based investigation only considered narrow collimated beams without overlapping and with no experimental verification.

In this paper, at first we introduce a detection technique based on DS that requires no CSI or a high computational load at the receiver. Then, we will show that under correlated-channels condition, the proposed DS scheme can deal with the variations of optimal DTL in turbulent channels. We also verify the analytical findings by experimental values. The rest of the paper is organized as follows. Section II describes the concept of differential signaling. Section III discusses the

Manuscript received XXX XX, 2015; one of the authors M. Mansour Abadi has a PhD scholarship from the Northumbria University. The work is also supported by the EU FP7 Cost Action IC1101.

The authors Mojtaba Mansour Abadi and Zabih Ghassemlooy are with Optical Communications Research Group, School of Computing, Engineering and Information Sciences, Northumbria University, Newcastle upon Tyne, NE1 8ST, U.K. (email: {mojtaba.mansourabadi, z.ghassemlooy}@northumbria.ac.uk)

Mohammad-Ali Khalighi is with the École Centrale Marseille, Institut Fresnel, UMR CNRS 7249, Campus de Saint-Jérôme, 13397 Marseille Cedex 20, France (e-mail: Ali.Khalighi@fresnel.fr).

Stanislav Zvanovec is with Department of Electromagnetic Field, Faculty of Electrical Engineering, Czech Technical University in Prague, 2 Technicka, 16627 Prague, Czech Republic (e-mail: xzvanove@fel.cvut.cz).

Manav R. Bhatnagar is with Department of Electrical Engineering Indian Institute of Technology Delhi, New Delhi, 110016, India (e-mails: manav@ee.iitd.ac.in).

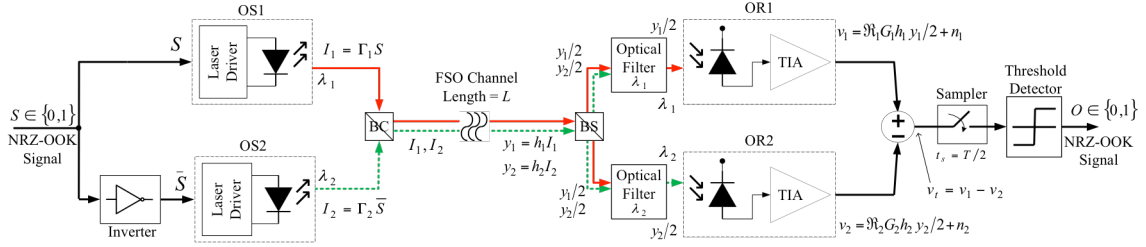


Fig. 1. The system block diagram to implement DS in correlated-channels conditions.  $T$  is the bit duration.

experimental campaign and results and section IV concludes the paper.

## II. DIFFERENTIAL SIGNAL TRANSMISSION

The proposed system block diagram is depicted in Fig. 1. The NRZ-OOK signal  $S \in \{0,1\}$  and its inverted version  $\bar{S}$  are used to intensity modulate two optical sources (OSs) at wavelengths of  $\lambda_1$  and  $\lambda_2$ , respectively. By comparing  $S$  to the optimal DTL  $S_{thresh} = E[S]$  where  $E[\cdot]$  denotes expected value, one can retrieve the original data bits (i.e., bit is 0 for  $S < S_{thresh}$  and 1 elsewhere). Note that the optimal DTL for  $\bar{S}$  is also  $S_{thresh}$ . The output intensities  $I_i$  ( $i = 1,2$ ) of OSs are given by

$$\begin{bmatrix} I_1 \\ I_2 \end{bmatrix} = \begin{bmatrix} \Gamma_1 & 0 \\ 0 & \Gamma_2 \end{bmatrix} \begin{bmatrix} S \\ \bar{S} \end{bmatrix} \quad (1)$$

where  $\Gamma_i$  denotes the electrical-to-optical conversion coefficient of OSs. The outputs of OSs are then passed through a beam combiner (BC) to ensure that both beams will be transmitted over the FSO channel of length  $L$ . Note that the BC is only used for alignment and not for combining signals in the optical domain. The optical signals  $\mathbf{y}$  at the receiver end are given by

$$\begin{bmatrix} y_1 \\ y_2 \end{bmatrix} = \begin{bmatrix} h_1 & 0 \\ 0 & h_2 \end{bmatrix} \begin{bmatrix} \Gamma_1 & 0 \\ 0 & \Gamma_2 \end{bmatrix} \begin{bmatrix} S \\ \bar{S} \end{bmatrix} \quad (2)$$

where  $h$  denotes the channel response including the effect of geometrical and atmospheric losses, pointing errors, and the AT. For simplicity, let us only consider the effect of AT. The optical signal is passed through a 50/50 beam splitter (BS) and optical filters (OF) with the centre wavelengths of  $\lambda_1$  and  $\lambda_2$ , prior to being collected by an optical receiver (OR). The generated photocurrents are amplified by transimpedance amplifiers (TIA) with outputs given by

$$\begin{bmatrix} v_1 \\ v_2 \end{bmatrix} = \frac{1}{2} \begin{bmatrix} \mathfrak{R}_1 G_1 h_1 \Gamma_1 & 0 \\ 0 & \mathfrak{R}_2 G_2 h_2 \Gamma_2 \end{bmatrix} \begin{bmatrix} S \\ \bar{S} \end{bmatrix} + \begin{bmatrix} n_1 \\ n_2 \end{bmatrix} \quad (3)$$

where  $\mathfrak{R}_i$  is the photodetector (PD) responsivity,  $G_i$  is gain of TIA,  $n_i$  is the additive white Gaussian noise (AWGN) with the zero mean and variance  $\sigma_{n,i}^2$ . The combined output  $v_t = v_1 - v_2$  is given by

$$v_t = \frac{1}{2} \Gamma_1 h_1 \mathfrak{R}_1 G_1 S - \frac{1}{2} \Gamma_2 h_2 \mathfrak{R}_2 G_2 \bar{S} + n_1 - n_2 \quad (4)$$

A sampler sampling at the centre of bit duration and a threshold detector are used to regenerate the transmit data. From (4), the optimal DTL for  $v_t$  is given by

$$V_{thresh} = \frac{1}{2} S_{thresh} (\Gamma_1 h_1 \mathfrak{R}_1 G_1 - \Gamma_2 h_2 \mathfrak{R}_2 G_2) + n_1 - n_2 \quad (5)$$

We have [10]

$$\text{Mean}(V_{thresh}) = \text{Mean}(h_1) - \text{Mean}(h_2) \quad (6a)$$

$$\text{Var}(V_{thresh}) =$$

$$\text{Var}(h_1) + \text{Var}(h_2) - 2\rho_{1,2} \sqrt{\text{Var}(h_1)\text{Var}(h_2)} + 2\sigma_n^2 \quad (6b)$$

where  $\text{Mean}(\cdot)$  denotes the average and  $\text{Var}(\cdot)$  introduces the variance. Here,  $\rho_{1,2}$  is correlation coefficient between the channels (i.e.,  $h_1$  and  $h_2$ ). For simplicity, we set  $\Gamma_1 \mathfrak{R}_1 G_1 = 2/S_{thresh}$  and  $\sigma_{n,1}^2 = \sigma_{n,2}^2 = \sigma_n^2$  in (6). For the weak AT regime  $h_i$  follows the log-normal distribution with mean and variance  $\mu_{h,i}$  and  $\sigma_{h,i}^2$ , respectively [10]. For log-normal distribution  $\text{Mean}(h_i) = \exp(\mu_{h,i} + \sigma_{h,i}^2/2)$  and  $\text{Var}(h_i) = (\exp(\sigma_{h,i}^2) - 1) \times \exp(2\mu_{h,i} + \sigma_{h,i}^2)$  where  $\mu_{h,i} = -\sigma_{h,i}^2$  [11]. Therefore,

$$\text{Mean}(V_{thresh}) = \exp(-\sigma_{h,1}^2/2) - \exp(-\sigma_{h,2}^2/2) \quad (7a)$$

$$\begin{aligned} \text{Var}(V_{thresh}) = & 2 - \exp(-\sigma_{h,1}^2) - \exp(-\sigma_{h,2}^2) - \\ & 2\rho_{1,2} \sqrt{1 - \exp(-\sigma_{h,1}^2)} \sqrt{1 - \exp(-\sigma_{h,2}^2)} + 2\sigma_n^2 \end{aligned} \quad (7b)$$

Since optical beams are in parallel and propagating very close to each other over the channel, then both beams will experience the same AT affects (i.e.,  $\sigma_{h,1}^2 \approx \sigma_{h,2}^2$ ). Considering this approximation, we obtain

$$\text{Mean}(V_{thresh}) = 0, \quad (8a)$$

$$\text{Var}(V_{thresh}) = 2(1 - \rho_{1,2})[1 - \exp(-\sigma_{h,1}^2)] + 2\sigma_n^2 \quad (8b)$$

Therefore, to recover the transmit bit stream, the optimal DTL should be set to 0. This is similar to the work in [2] with the difference that the authors did not take into account the variance of the detection threshold in (8b), which results from AT. However, for  $\rho_{1,2} = 1$  (i.e., the highly correlated channels), we have  $\text{Var}(V_{thresh}) = 2\sigma_n^2$ . In other words, AT does not impact signal detection. According to [12], in the weak AT regime  $\rho_{1,2}$  can be expressed in terms of the transversal distance between the receiver apertures  $d_r$  and the spatial coherence radius  $\rho_0$ . Here, with parallel optical beams propagating over a line-of-sight (LOS),  $d_r$  is in fact the distance between the propagation axes of beams. Thus the correlation coefficient between channels takes the form of [12]

$$\rho_{1,2} = \exp \left[ - \left( \frac{d_r}{\rho_0} \right)^{5/3} \right] \quad (9)$$

where for a plane wave propagation model  $\rho_0$  is given by [13]

$$\rho_0 = \left( 1.455 \left( \frac{2\pi}{\lambda} \right)^2 C_n^2 L \right)^{-3/5} \quad (10)$$

where  $C_n^2$  (in unit of  $\text{m}^{-2/3}$ ) is the refractive index structure coefficient, which gives an indication of the AT strength [11]. From (9), for  $(d_r/\rho_0)^{5/3} > 5$  channels are considered uncorrelated  $\rho_{1,2} < 0.007$  whilst for  $d_r \rightarrow 0$  we obtain  $\rho_{1,2} \rightarrow 1$ . So, by adopting a small  $d_r$ , we can obtain highly correlated channels and, as a result, use an optimal DTL independent of AT. In the next section we will outline the experimental work for the proposed system given in Fig. 1.

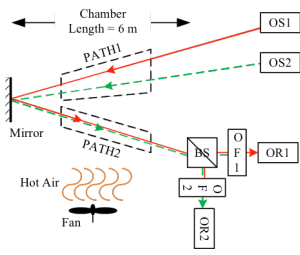
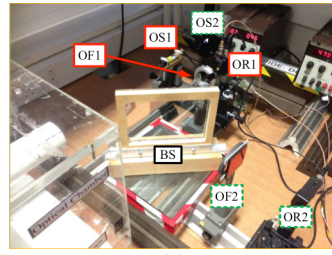
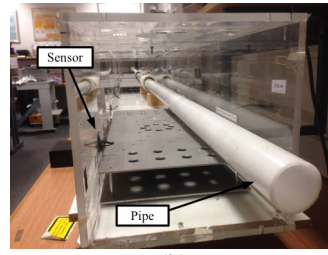


Fig. 2 Block diagram of the experimental setup.



(a)



(b)

Fig. 3 Experimental setup snapshot: (a) transmitters and receivers at one end of the chamber and (b) atmospheric chamber with temperature sensors to measure temperature gradient, and a pipe to isolate either PATH1 or PATH2 from the turbulence conditions in the chamber.

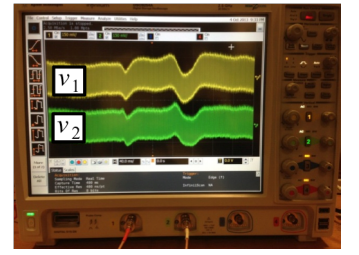


Fig. 4 Original ( $v_1$  in yellow and top) and inverted ( $v_2$  in green and bottom) signals captured on the oscilloscope.

### III. EXPERIMENTAL MEASUREMENTS

According to proposed scheme in Fig. 1, we have developed an experimental setup to evaluate the performance of the proposed method by generating the conditions of both uncorrelated (i.e.,  $\rho_{1,2} = 0$ ) and correlated (i.e.,  $\rho_{1,2} \rightarrow 1$ ) channels as depicted in Fig. 2. Snapshots of the setup are also shown in Fig. 3. The laser beams from OSs (Fig. 3(a)) were launched into a chamber of length 6 m, emulating an outdoor uncorrelated FSO channel (Fig. 3(b)). We denote the incident and reflected ray paths by PATH1 and PATH2, respectively (see Fig. 2). Based on the theory of beam propagation through a random medium we determined the minimal transverse coherence distance  $d_{tc}$ , to ensure uncorrelated received signals. Values of  $d_{tc}$  were derived from measured distributions of the thermal structure parameter  $C_n^2$  (obtained from  $C_n^2$ ) along optical beams according to [14]. Alternatively, an expression for beam separation can also be set by the scintillation anisoplanatic distance [15]. In PATH1 OSs were spaced apart by a minimum distance of  $d_r > 5$  mm to ensure uncorrelated fading conditions (i.e.,  $(d_r/\rho_0)^{5/3} > 5$ ). An adjustable mirror positioned at the other end of the chamber was used to increase the path length by reflecting back the beams. The reflected beams indicated by PATH2 in Fig. 2 were kept as close as possible to each other to ensure high correlation between the two paths (note that PATH2 in Fig. 2 corresponds to FSO channel in Fig. 1). Heater fans were used to generate AT in the chamber, see Fig. 2. To measure  $C_n^2$ , we used the method of thermal structure parameter (based on temperature gradient measurement) as in [16]. The temperature gradient was measured using 20 temperature

TABLE I THE EXPERIMENTAL SETUP PARAMETERS

	Parameter	Value
	Data rate NRZ-OOK	100 kbps
	Chamber length $L$	6 m
Link 1	Optical transmit power	10 dBm
	Divergence angle	9.5 mDeg
	PD responsivity $\mathcal{R}_1$	0.3 A/W
	Wavelength $\lambda_1$	830 nm
Link 2	Optical transmit power	3 dBm
	Divergence angle	4.8 mDeg
	PD responsivity $\mathcal{R}_2$	0.4 A/W
	Wavelength $\lambda_2$	670 nm
	OR noise rms $\sqrt{\sigma_n^2}$	1.5 mV

sensors positioned along the chamber, see Fig 3(b). At the receiver end the reflected beams passed through a 50/50 BS and were applied to two identical PIN PDs after OFs, see Figs. 2 and 3(a). The outputs of PDs were captured using a real-time digital storage oscilloscope for further processing by MATLAB<sup>®</sup>.

We first investigated the effect of AT on the uncorrelated path within the chamber. The reflected beams (i.e., PATH2) were passed through a pipe positioned within the chamber. The pipe ensured that propagating beams inside it did not experience any AT, see Fig. 3(b). Similarly, we investigated the effect of AT on the correlated path by isolating the uncorrelated channels (i.e., optical beams in PATH1 propagating through the pipe), see Fig. 2. We set the amplitudes of  $S$  and  $\bar{S}$  in order to ensure that both received electrical signals  $v_1$  and  $v_2$ , have the same amplitude of  $\sim 300$  mV, which is equivalent to  $\Gamma_1 \mathcal{R}_1 G_1 = \Gamma_2 \mathcal{R}_2 G_2$  criterion. Table I shows all the key parameters adopted in our experiment.

The measured mean and standard deviation of  $V_{thresh}$  (indicated by Mean and  $\sqrt{\text{Var}}$  respectively) as well as  $C_n^2$  values for correlated and uncorrelated channels are summarized in Table II. As predicted from (8a), for both uncorrelated and correlated conditions the measured mean value is zero. However, the variance of  $V_{thresh}$  is reduced in correlated channels case, which is in good agreement with (8(b)). Fig. 4 shows an image taken from the oscilloscope screen illustrating how signals  $v_1$  and  $v_2$  for correlated channels are affected under the same AT conditions. Note that AT strength and the laser modulation index in Fig. 4 were deliberately set to relatively small values in order to better illustrate correlation between  $v_1$  and  $v_2$ . We would expect to obtain  $\sqrt{\text{Var}} \approx \sqrt{2\sigma_n^2}$  from our measurements. However, given the rms noise of OR in Table I, the measured  $\sqrt{\text{Var}}$  in Table II is different from the predicted value of  $\sqrt{2\sigma_n^2} =$

TABLE II SUMMARY OF THE EXPERIMENTAL MEASUREMENT RESULTS

Channels condition	Mean (mV)	$\sqrt{\text{Var}}$ (mV)	$C_n^2$ ( $\text{m}^{-2/3}$ )	$\rho_{1,2}$
Uncorrelated (dark room)	0.0	43.4	$5.11 \times 10^{-11}$	0.08
Uncorrelated (lit room)	0.0	45.5		
Correlated (dark room)	0.0	12.9	$5.21 \times 10^{-11}$	0.72
Correlated (lit room)	0.0	12.9		

2.1 mV. This difference can be due to imperfect correlation between channels in PATH2 and the fact that two (not very close) wavelengths of 670 and 830 nm we used could lead to dissimilar  $\sigma_h^2$ . For a plane wave propagation in a AT channel  $\sigma_h^2$  is given by [11]

$$\sigma_h^2 = 0.3075 \left(\frac{2\pi}{\lambda}\right)^{\frac{7}{6}} L^{\frac{11}{6}} C_n^2 \quad (11)$$

Also another term called Rytov variance  $\sigma_R^2 = 4\sigma_h^2$  can be used to indicate the strength of AT [15]. In our experiment  $\sigma_R^2 \approx 0.17$ , which corresponds to weak AT regime [15].

To qualify the requirement for using light sources with very close wavelengths, let us take the derivate of (11) with respect to the wavelength, which gives  $\Delta\sigma_h^2 = \frac{7}{6}\sigma_h^2 \Delta\lambda/\lambda_0$  where  $\lambda_0 = (\lambda_1 + \lambda_2)/2$  and  $\Delta\lambda = |\lambda_1 - \lambda_2|$ . Using the rule of thumb, to have  $\Delta\sigma_h^2/\sigma_h^2 < 0.1$ , we should have  $\Delta\lambda/\lambda_0 < 0.09$ . Note that in our experiment, the accuracy limit of (8b) does not apply perfectly (as we have  $\Delta\lambda/\lambda_0 < 0.21$ , which corresponds to a maximum wavelength deviation of 160 nm around the central wavelength of 750 nm). Using measured signals we estimated  $\rho_{1,2}$ , which are presented in Table II. The estimated  $\rho_{1,2}$  (for the correlated case) are relatively high but do not correspond to the ideal case of  $\rho_{1,2} = 1$ . Other effects that could lead to inaccuracy of the measurement were the noise associated with the oscilloscope and the vibration of the whole setup. However since we intended to demonstrate only the difference between uncorrelated and correlated situations and during the entire measurement the same setup was used, these effects are not critical in the final conclusion. In addition to closer wavelength and spatially closer beams, From (10) it is evident that longer transmission spans will lead to larger values of  $\rho_0$ , which in turn helps to achieve a highly correlated-channels condition (i.e.,  $\rho_{1,2} \rightarrow 1$ ) [17].

In [9], a similar DS-based technique was proposed to reduce the effect of background noise in the received signal. We carried out the above experiment in both dark and fully lit environments (with ambient light power level of  $-45$  dBm and  $-18$  dBm, respectively), see Table II. We notice a negligible difference between the results in these two cases. This testifies that under the experimental conditions that we carried out the measurements, the background noise was not the dominant. Thus reduction in  $\sqrt{\text{Var}}$  values is due to the theory explained in Section II rather than a reduction in the background noise level.

#### IV. CONCLUSIONS

The paper proposed a detection technique based on differential signaling that does not require CSI at the receiver, thus no pilot overhead or any noticeable increase in the receiver computational complexity. Using the derived analytical expression of the variance of the detection threshold, it was shown that the fluctuation in the optimal DTL highly depended on the correlation between the propagating optical beams. Thus the proposed technique is attractive when we can establish highly correlated FSO channels. This deduction was validated by means of experimental investigations under uncorrelated and correlated

conditions. Also it was discussed that to achieve a high correlated-channel condition, closer wavelength, spatially closer beams and longer transmission distance are critical.

#### ACKNOWLEDGMENT

One of the authors M. Mansour Abadi has received a PhD scholarship from the Northumbria University. The work is also supported by the EU FP7 Cost Action IC1101.

#### REFERENCES

- [1] S. Tianyu and K. Pooi-Yuen, "A robust GLRT receiver with Implicit channel estimation and automatic threshold adjustment for the free space optical channel with IM/DD," *Lightwave Technology, Journal of*, vol. 32, pp. 369-383, 2014.
- [2] S. Hitam, M. Abdullah, M. Mahdi, H. Harun, A. Sali, and M. Fauzi, "Impact of increasing threshold level on higher bit rate in free space optical communications," *Journal of Optical and Fiber Communications Research*, vol. 6, pp. 22-34, 2009/12/01 2009.
- [3] Z. Ghassemlooy, S. Rajbhandari, and W. Popoola, *Optical wireless communications: system and channel modelling with MATLAB*. Boca Raton, FL: Taylor & Francis, 2013.
- [4] M. A. Khalighi and M. Uysal, "Survey on Free Space Optical Communication: A Communication Theory Perspective," *Communications Surveys & Tutorials, IEEE*, vol. 16, pp. 2231-2258, 2014.
- [5] X. Zhu and J. M. Kahn, "Free-space optical communication through atmospheric turbulence channels," *Communications, IEEE Transactions on*, vol. 50, pp. 1293-1300, 2002.
- [6] X. Zhu and J. M. Kahn, "Markov chain model in maximum-likelihood sequence detection for free-space optical communication through atmospheric turbulence channels," *Communications, IEEE Transactions on*, vol. 51, pp. 509-516, 2003.
- [7] X. Zhu and J. M. Kahn, "Pilot-symbol assisted modulation for correlated turbulent free-space optical channels," in *Proc. SPIE 4489, Free-Space Laser Communication and Laser Imaging*, 2002, pp. 138-145.
- [8] M. L. B. Riediger, R. Schober, and L. Lampe, "Fast multiple-symbol detection for free-space optical communications," *Communications, IEEE Transactions on*, vol. 57, pp. 1119-1128, 2009.
- [9] M. A. Khalighi, F. Xu, Y. Jaafar, and S. Bourennane, "Double-laser differential signaling for reducing the effect of background radiation in free-space optical systems," *Optical Communications and Networking, IEEE/OSA Journal of*, vol. 3, pp. 145-154, 2011.
- [10] A. Leon-Garcia, *Probability and random processes for electrical engineering*. Reading, Mass: Addison-Wesley, 1989.
- [11] S. M. Navidpour, M. Uysal, and M. Kavehrad, "BER performance of free-space optical transmission with spatial diversity," *Wireless Communications, IEEE Transactions on*, vol. 6, pp. 2813-2819, 2007.
- [12] G. R. Osche, *Optical Detection Theory for Laser Applications*. New York: Wiley, 2002.
- [13] M. A. Khalighi, N. Schwartz, N. Aitamer, and S. Bourennane, "Fading reduction by aperture averaging and spatial diversity in optical wireless systems," *Optical Communications and Networking, IEEE/OSA Journal of*, vol. 1, pp. 580-593, 2009.
- [14] J. A. Louthain and J. D. Schmidt, "Anisoplanatism in airborne laser communication," *Optics Express*, vol. 16, pp. 10769-10785, 2008/07/07 2008.
- [15] L. C. Andrews and R. L. Phillips, *Laser Beam Propagation through Random Media*, Second Edition (SPIE Press Monograph Vol. PM152): SPIE Publications, 2005.
- [16] Z. Ghassemlooy, H. Le Minh, S. Rajbhandari, J. Perez, and M. Ijaz, "Performance analysis of ethernet/fast-ethernet free space optical communications in a controlled weak turbulence condition," *Lightwave Technology, Journal of*, vol. 30, pp. 2188-2194, 2012.
- [17] G. Yang, M. A. Khalighi, S. Bourennane, and Z. Ghassemlooy, "Fading correlation and analytical performance evaluation of the space-diversity free-space optical communications system," *Journal of Optics*, vol. 16, p. 035403, 2014.